Neural Computing and Applications (2020) 32:15687–15697
https://doi.org/10.1007/s00521-018-3443-z

S.I. : ADVANCES IN BIO-INSPIRED INTELLIGENT SYSTEMS

Automatic computer vision-based detection and quantitative analysis of indicative parameters for grading of diabetic retinopathy

Ashish Issac[1] · Malay Kishore Dutta[1] · Carlos M. Travieso[2]

Received: 19 December 2017 / Accepted: 16 March 2018 / Published online: 21 March 2018

Abstract
Diabetic retinopathy (DR) is one of the complications of diabetes affecting the eyes. If not treated at an early stage, then it can cause permanent blindness. The present work proposes a method for automatic detection of pathologies that are indicative parameters for DR and use them strategically in a framework to grade the severity of the disease. The bright lesions are highlighted using a normalization process followed by anisotropic diffusion and intensity threshold for detection of lesions which makes the algorithm robust to correctly reject false positives. SVM-based classifier is used to reject false positives using 10 distinct feature types. Red lesions are accurately detected from a shade-corrected green channel image, followed by morphological flood filling and regional minima operations. The rejection of false positives using geometrical features makes the system less complex and computationally efficient. A comprehensive quantitative analysis to grade the severity of the disease has resulted in an average sensitivity of 92.85 and 86.03% on DIARETDB1 and MESSIDOR databases, respectively.

Keywords Fundus images · Diabetic retinopathy · Optic disc · Bright lesions · Red lesions · Mathematical morphology · Classification · Grading

1 Introduction

Diabetic retinopathy (DR) is a disease related to retina of the human eye. This disease can cause permanent blindness to the affected person if proper treatment is not granted at an early stage. In developing countries, there is a scarcity of trained ophthalmologists and lack of awareness about such diseases. However, if proper awareness creation camps and some automated tools are developed, then some initial care can be given to patients and the progression of the disease can be delayed.

The disease is mainly characterized by the presence of lesions, either bright or red, on the retina, venous beading and neo-vascularization. However, with the help of image processing, the visual changes observed in the retina can be detected and some algorithms can be developed to detect these abnormalities. Development of computer-aided tools for detection of DR has been critically important considering the lack of awareness and scarcity of ophthalmologists. Various lesions show changes in colour, geometrical features and texture features, and detection can be made less complex and computationally efficient using imaging techniques.

Some scientific work is reported in the computer-aided detection of DR using image processing. Roychowdhury et al. [1] have proposed the use of various classification techniques for analysis of lesions in a fundus image. Seoud et al. [2] have proposed the use of some set of features and named them as dynamic shape features for detection of red lesions and haemorrhages from fundus images. Issac et al. [3] have proposed a method for optic disc segmentation

✉ Malay Kishore Dutta
mkdutta@amity.edu

Ashish Issac
aissac@amity.edu

Carlos M. Travieso
carlos.travieso@ulpgc.es

1 Department of Electronics and Communication Engineering, Amity University, Noida, India

2 Signals and Communication Department, IDeTIC, University of Las Palmas de Gran Canaria, Las Palmas de Gran Canaria, Spain

which involves successive subtraction of statistical features followed by intensity-based adaptive thresholding for optic disc segmentation. Finally, some structural and clinical features were fed to a classification module for identification of glaucoma from fundus images. Franklin and Rajan [4] have proposed the use of artificial neural network for classification of exudates using colour, size, shape and textural features for DR detection in fundus images. Ranamuka and Meegama [5] have proposed the use of morphological operations and fuzzy logic for detection of exudates from fundus images for analysis of DR. Sengar and Dutta [6] have proposed a hierarchical model for grading a fundus image for severity of diabetic retinopathy. The lesions have been segmented using intensity-based thresholding and morphological operations. Some geometrical features have been used to differentiate between microaneurysms and haemorrhages. Antal and Hajdu [7] have proposed an ensemble-based approach to improve the accuracy of microaneurysms detection. Ram et al. [8] have proposed the use of successive rejection-based strategy to remove the false positives for microaneurysms detection from fundus images. Parthasarathi et al. [9] have proposed an adaptive region growing-based method for optic disc segmentation from a blood vessel inpainted fundus image. Singh et al. [10] have proposed the use of wavelet features for identification of glaucoma from fundus images. The optic disc has been segmented using a blood vessel inpainting and region growing technique. Yadav et al. [11] have proposed the use of neural network for classification of glaucoma from fundus images. Zhang et al. [12] have proposed the use of a modified matched filter for identification of neo-vascularization to detect signs of proliferative DR from fundus images. Osareh et al. [13] have proposed the use of fuzzy c-means clustering and colour, size, edge and texture-based features for detection of exudates from the fundus images. Ganguly et al. [14] have proposed the use of an adaptive threshold for detection and differentiation of red lesions from blood vessels. Dutta et al. [15] have proposed a diagnostic method for detection and grading of severity of diabetic retinopathy. A region-based approach has been used to grade the severity of the disease. Soorya et al. [16] have proposed a vessel bending-based approach to identify the boundary of optic cup in a fundus image. The bending-based method is clinically viable and accepted across the globe by ophthalmologists. Although some work has been done in the past, there exists a need for more robust and computationally efficient computer-based method which can perform real-time detection of DR from fundus images.

The main contribution of the proposed method is the use of distinctive features for classification of bright lesions and correctly rejects false positives. Some aberrations which get introduced during the image acquisition process might result in false detections and hamper the accuracy of DR detection. These false detections might resemble exudates with respect to colour and intensity. However, the proposed system has strategically used statistical, geometrical and location-dependent features for correct detection of exudates from fundus images. The segmentation results are encouraging and able to correctly reject false candidate objects using the proposed method.

Another significant contribution of the proposed method is the use of shape-based features for detection of red lesions from fundus images. The correct rejection of blood vessels detected along with the red lesions becomes important. The blood vessels have distinctive characteristics with respect to geometry as compared to red lesions. This property has been used as a basis to develop a geometrical and intensity-based effective framework to reject false positives in the proposed work.

The remaining paper is structured as follows: Sect. 2 discusses the image processing techniques used in the proposed work for localization of optic disc and segmentation of lesions. The section also discusses the framework for grading of the disease which is derived from clinically accepted rule. Section 3 discusses the experimental results and Sect. 4 discusses the conclusions.

2 Proposed methodology

A normal fundus image consists of foreground objects like optic disc, blood vessels and macula. However, if a person is suffering from diabetes, then the effect of the disease can be seen on the eyes. Diabetic retinopathy is one of the complications of diabetes and is characterized by the presence of various abnormalities in a fundus image. The walls of the blood capillaries become weak, and secretion occurs which results in accumulation of blood and lipids on the retina and is categorized as red and bright lesions, respectively. The various abnormalities and objects present in a fundus image are shown in Fig. 1.

In the proposed method, a strategic framework has been developed to detect the presence of objects and abnormalities present in a fundus image and use them to perform a quantitative and qualitative analysis to grade the severity of the disease. A graphical representation of the image processing methods and techniques used in the proposed work is summarized and shown in Fig. 2. The entire process can be divided into four major steps:

1. Optic disc segmentation and removal.
2. Bright lesions (exudates) segmentation and classification.
3. Red lesions (haemorrhages and microaneurysms) segmentation and classification.

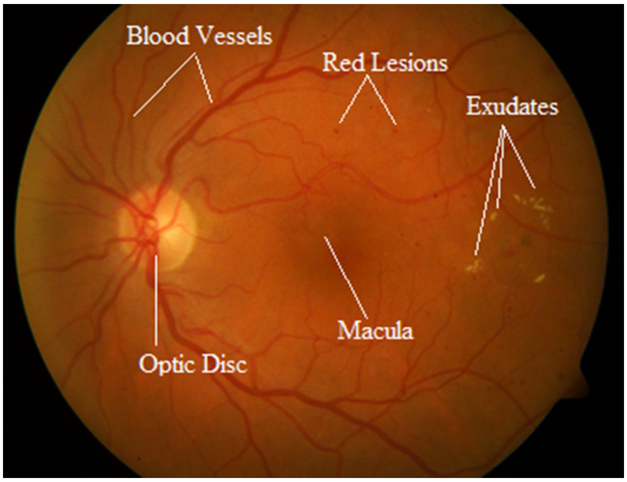

Fig. 1 Labeled fundus image

4. Framework for quantitative analysis of fundus images.

2.1 Optic disc segmentation and removal

Optic disc is an important object present in the fundus image. Correct detection of optic disc in fundus image is significant in correct diagnosis of many diseases. In the proposed work, an imaging method is proposed to localize the optic disc in a fundus image by determining the pixels with high intensity. The optic disc is localized from the greyscale image. The input image in RGB format is decomposed into its components—red, green and blue. A weighted sum of all three channels is performed to produce a greyscale image using Eq. 1.

$$\mathrm{Ig} = 0.2989 * \mathrm{R} + 0.5870 * \mathrm{G} + 0.1140 * \mathrm{B} \tag{1}$$

where Ig = greyscale image, R = red channel image, G = green channel image, B = blue channel image.

Once the greyscale image is obtained, the image is smoothed using an averaging filter. It has been observed that optic disc represents the pixels corresponding to high intensities in the fundus images. So, on applying smoothing filter, the intensities are uniformed, while the high-intensity pixels appear distinct than the background pixels. The size of the filter plays a key factor in correct localization of the optic disc. The size of the filter should be kept equal to that of the optic disc so that other pixels of high intensity are not localized as optic disc pixels. So, an averaging filter of empirical value of 51 pixels has been selected to blur the image. After observing many fundus images, it was observed that the radius of optic disc is approximately equal to this empirical value.

Since OD corresponds to the high-intensity pixels, a pixel of highest intensity is searched in the average filtered image. If multiple points are detected, then an average of such points is considered. Depending on the location of the optic disc obtained using the high-intensity method, this coordinate is shifted by a few pixels depending on whether the image belongs to left or right eye. Finally, a circle of some radius is created with this coordinate as centre and this portion is termed as optic disc. This optic disc is eliminated from the exudates and haemorrhages final images to remove false positives. The process of OD segmentation is explained in Fig. 3.

2.2 Bright lesion (exudates) segmentation and classification

Bright lesions are categorized into hard exudates and cotton soft wools. The secretion of proteins or lipids from the blood capillaries results in the accumulation of yellow-coloured structures on the retina and is termed as bright lesions. This is so because they appear as bright objects and constitutes as pixels with high intensities in fundus image when captured using a high-resolution digital camera. In the proposed method, a normalized green channel of the fundus image has been used for exudates segmentation. The green channel is subjected to anisotropic diffusion [17], and the updated image is thresholded to yield pixels which are possible candidates for exudates. The candidate pixels contain many false positives, in the form of either optic disc or reflections introduced during image acquisition. The optic disc is localized by determining a pixel of

Fig. 2 Graphical representation of imaging techniques used in the proposed work

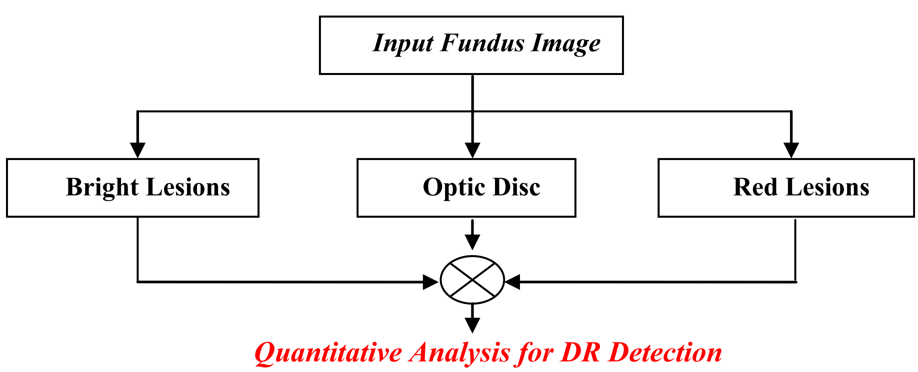

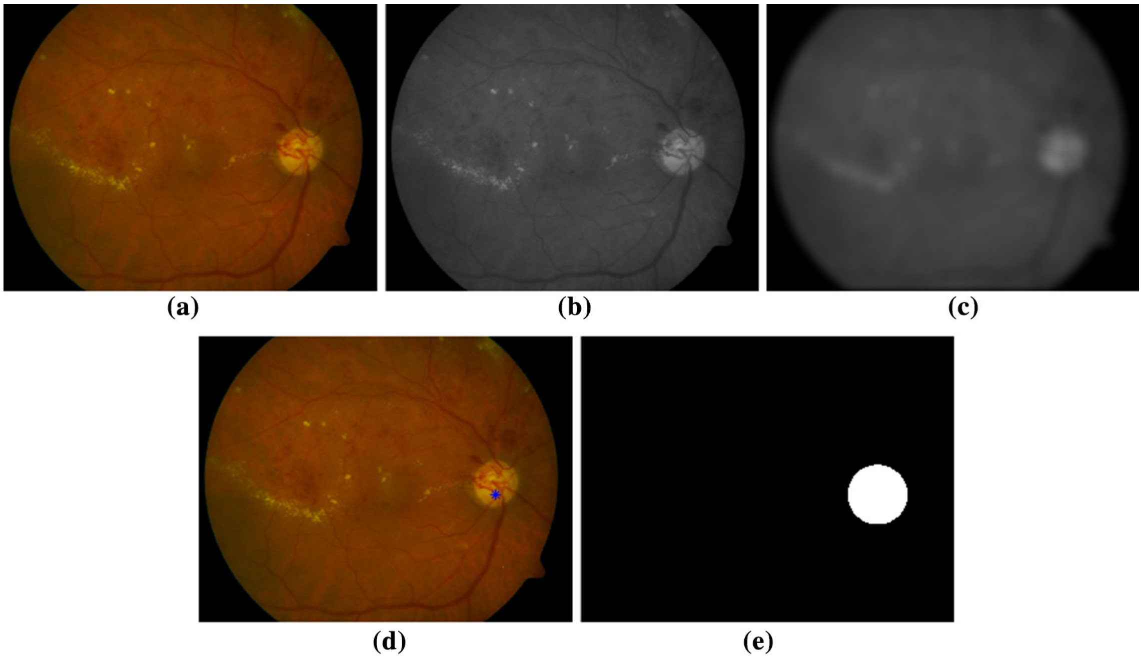

Fig. 3 Optic disc localization and segmentation **a** input image, **b** greyscale image, **c** average filter smoothed greyscale image, **d** optic disc centre marked on input image, **e** circular mask which will be used to remove OD pixels

maximum intensity from a highly smoothed fundus image. Once the optic disc is removed from the output image, the resultant image is used for feature extraction and classification for rejection of false positives. The imaging methods and techniques used for exudates segmentation and classification are summarized graphically in the form of a block diagram and shown in Fig. 4.

2.2.1 Exudates (candidate pixels) segmentation

The input fundus image is in RGB format and constitutes of three basic channels, namely red, green and blue. During the image acquisition process, some noise gets introduced in the image which can result in uneven colour and brightness. Such variations in colour and brightness can cause alterations in the fundus images which needs to be nullified to obtain better results during object segmentation. So, a brightness and colour correction method is applied on the input image to normalize the effect of such variations.

The input fundus image in RGB colour space is first converted to HSV colour space. The V-channel of HSV image is extracted and normalized as per Eq. 2:

$$\mathrm{V}_{\mathrm{new}} = \sqrt[2]{1 - (\mathrm{V} - 1)^2} \tag{2}$$

The updated normalized v-channel is combined with the original H and S-channel to produce a new image in HSV format. The new HSV image is converted back to RGB colour space and decomposed to extract the green channel. Due to the even distribution introduced due to the normalization process, objects like blood vessels, haemorrhages and exudates become clearly visible in the updated green channel, which is ultimately used for exudates segmentation. Figure 5 shows the normalization process used in the work for brightness and colour correction in the fundus image.

The extracted green channel is subjected to anisotropic diffusion [17]. Anisotropic diffusion is an imaging technique which is helpful in minimizing the noisy pixels while retaining the information containing pixels in an image. The information containing pixels corresponds to a line or edge in an image. The input image is combined with a filter which can very itself according to the local distribution in the image. This results in an output image which is nonlinearly filtered. Thus, anisotropic diffusion process can be called as space variant transformation of an image.

The basic idea of using anisotropic diffusion is to retain the edges of the exudates while smoothing the retinal background. The intensities in the background are smoothed, and when subtracted from the original image, it results in the pixels with high intensities, i.e. exudates candidate pixels. The resulting image is subjected to intensity-based threshold which ultimately results in a binary image consisting of exudates and some false positives. The intensity-based threshold is determined by performing a histogram analysis of the subtracted image. The threshold is determined by using some features from the image itself so that correct segmentation occurs for each image. This makes the threshold process adaptive and

Fig. 4 Block diagram for exudates segmentation and classification

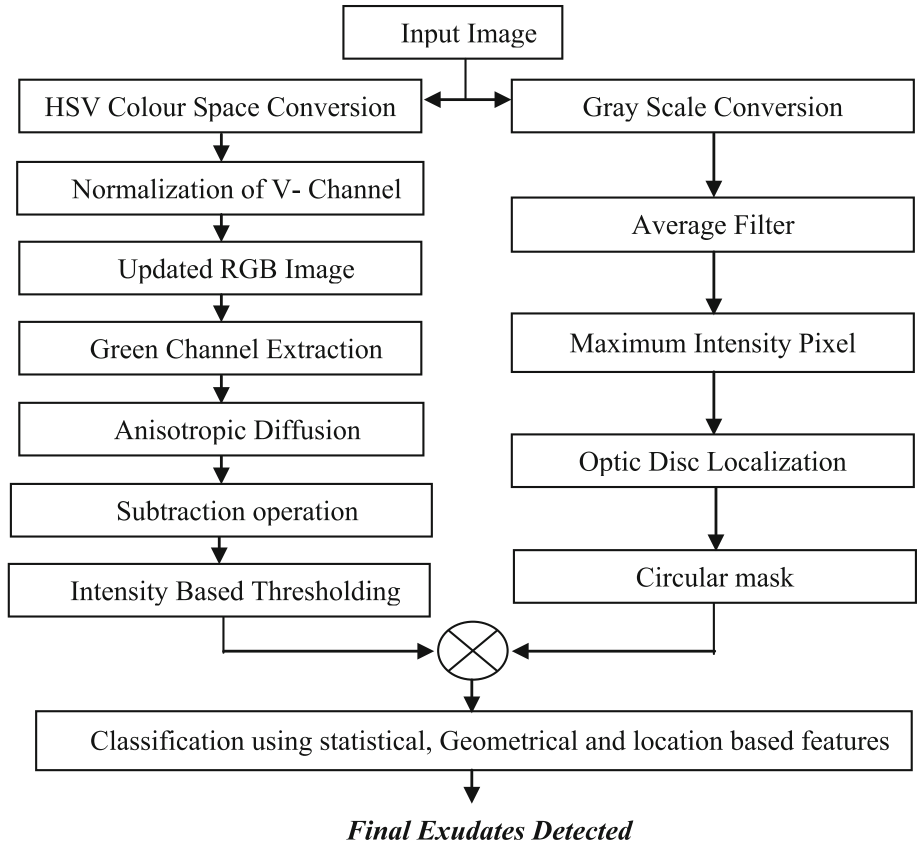

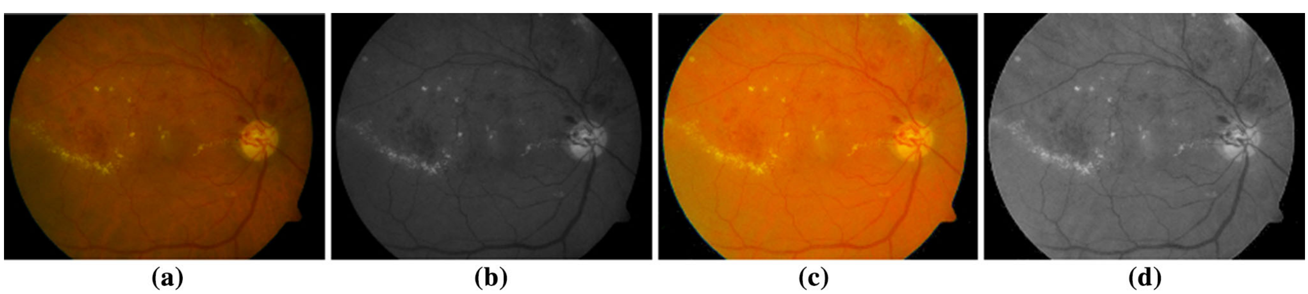

Fig. 5 Brightness and colour correction **a** original input image, **b** green channel of original input image, **c** normalized image, **d** green channel of normalized image

independent of any other image in the database. Equation 3 represents the threshold used for binarizing operation.

$$T1 = [(a * \mu(s)) + (b * \sigma(s))] \tag{3}$$

where T1 is the adaptive threshold for segmentation of high-intensity pixels, s is the subtracted image, a and b are the weights, and μ and σ represent the mean and standard deviation, respectively.

The process of applying anisotropic diffusion to the green channel, subtraction and intensity-based thresholding is shown in Fig. 6.

2.2.2 Classification for accurate exudates segmentation

Figure 6 shows that the final image obtained post-thresholding consists of some false positives. These false positive pixels consist of pixels belonging to optic disc and reflections. Removal of such pixels becomes an important task in correctly identifying the pixels pertaining to some abnormality. Feature extraction for all the objects obtained in the binary image post-thresholding is performed to differentiate between actual exudates and false positive pixels. For this purpose, a statistical, geometrical and location-dependent features-based framework is developed and fed to a classification module.

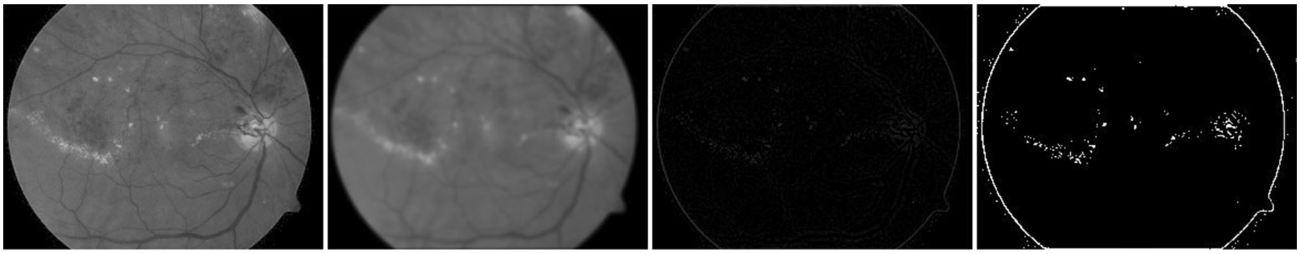

Fig. 6 Anisotropic diffusion, **a** green channel, **b** anisotropic diffusion subjected image, **c** subtraction process, **d** intensity-based thresholding

Table 1 Features for rejection of false positives in case of bright lesions

S no.	Feature name	Feature type	Approach
1	Mean	Statistical	Difference in intensity
2	Standard deviation	Statistical	Difference in intensity
3	Variance	Statistical	Difference in intensity
4	Area	Geometrical	Difference in size determined by no. of white pixels
5	Perimeter	Geometrical	Difference in size determined by objects boundary
6	Solidity	Geometrical	Difference in size determined by measuring the no of holes
7	Eccentricity	Geometrical	Difference in size determined by measuring how elliptical an object is
8	Aspect ratio	Geometrical	Difference in size determined by the ratio of major to minor axis
9	Distance from OD	Location dependent	Location of object in image
10	Slope from OD	Location dependent	Location of object in image

A total of 10 distinct features are considered to determine the difference between the finally obtained objects. These features are discussed in Table 1.

These multiple and distinct features are extracted for every object and fed to a classification module to identify whether the object belongs to an exudate or false positive class. The classification module used in the proposed work is a support vector machine (SVM) based on supervised learning environment. SVM is a binary classifier capable of separating samples in a multi-dimensional space using a hyperplane. The training vector consists of the discussed features for only exudates and only reflections. When a new fundus image is tested using this classifier, the classifier successfully rejects the pixels corresponding to reflections and correctly retains exudate pixels in the image. This is shown in Fig. 7.

2.3 Red lesions segmentation and classification

2.3.1 Shade correction

The green channel of original fundus image is considered for red lesions segmentation as it has the highest contrast among the three channels between lesions and background. Due to the image acquisition process, there may be some illumination variations in the captured fundus image. So, a shade correction technique is implemented to correct the uneven illumination problem. A polynomial fitting-based shade correction technique is used in the proposed work [18]. The shade correction is based on the notion that the luminance can be expressed as product of shading and reflectance. Mathematically this is expressed as Eq. (4):

$$\mathrm{I} = \mathrm{R} * \mathrm{S} \tag{4}$$

$$\mathrm{R} = k * (\mathrm{I} / \mathrm{S}) \tag{5}$$

where I = luminance image, R = reflectance image, S = shading image, k = scaling factor representing mean luminance of test image.

An intermediate shading image is obtained by fitting least square curves for each row and column. The original green channel image is divided by this shading image and multiplied by a constant to obtain a restored shade-corrected image. The process is shown in Fig. 8.

2.3.2 Red lesions segmentation

The shade-corrected green channel image is used for red lesion segmentation from the fundus images. The image is subjected to a median filtering operation in order to remove some noisy pixels which might represent spikes. The filtered image is subjected to a flood-fill operation in which the pixels having intensity below a level are replaced by mean intensity. The filtered image is subtracted from the flood-filled image to result in pixels with low intensities in

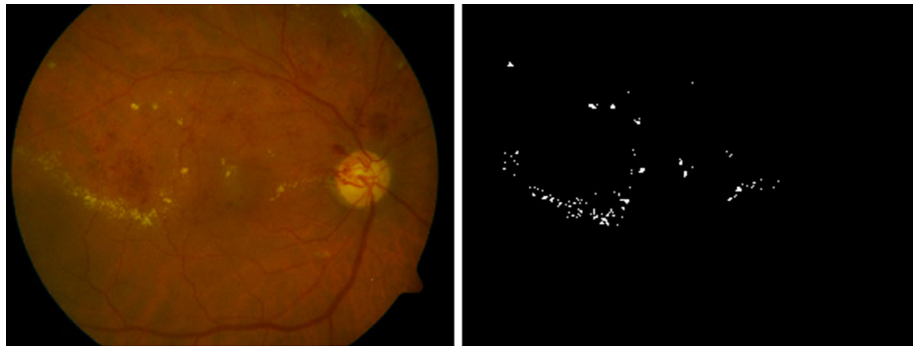

Fig. 7 Classification of exudates

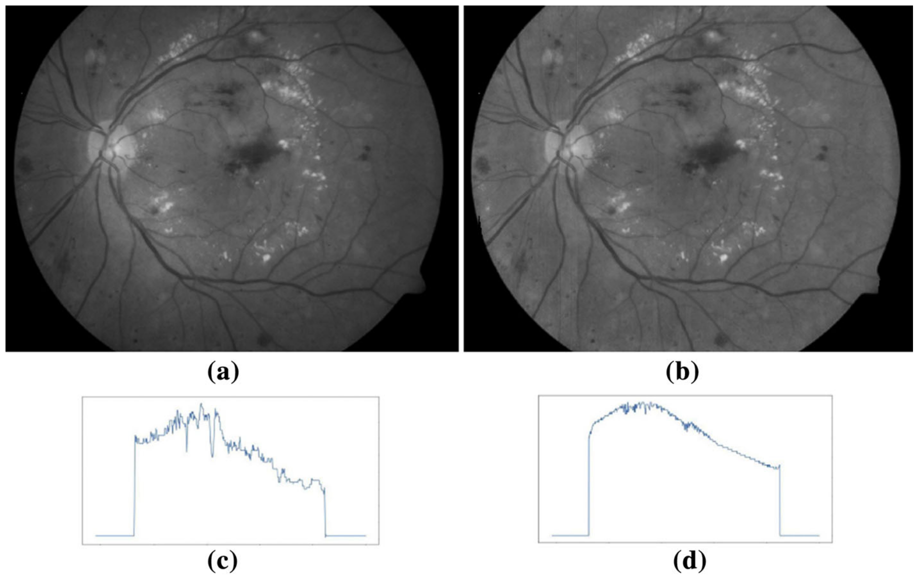

Fig. 8 Shade correction **a** green channel, **b** shade-corrected green channel, **c** intensity plot of a row in original green channel, **d** intensity plot of same row in shade-corrected green channel

the image. Now, the resultant image is subjected to a regional minima operation. These regional minima pixels are dark pixels and correspond to red lesions, macula or blood vessels. The segmentation process is shown in Fig. 9.

The objects present in the resulting image may differ in geometrical properties. So, a geometrical property-based framework is designed to segment only the red lesions and reject blood vessels to improve the accuracy. The blood vessels segmented in the resulting image are observed to be larger as compared to the red lesions. So, only those objects whose major-to-minor axis ratio is less than 1.8 are retained. The resulting image may have some background pixels which are to be removed. The lesion pixels are much darker than the background pixels, so an intensity-based threshold is applied to remove more noisy pixels. As a decisive step, circularity of the objects is determined to eliminate some smaller vessels. The final image consists of red lesions, which will be used to determine the severity of the disease. The above process is shown in Fig. 10.

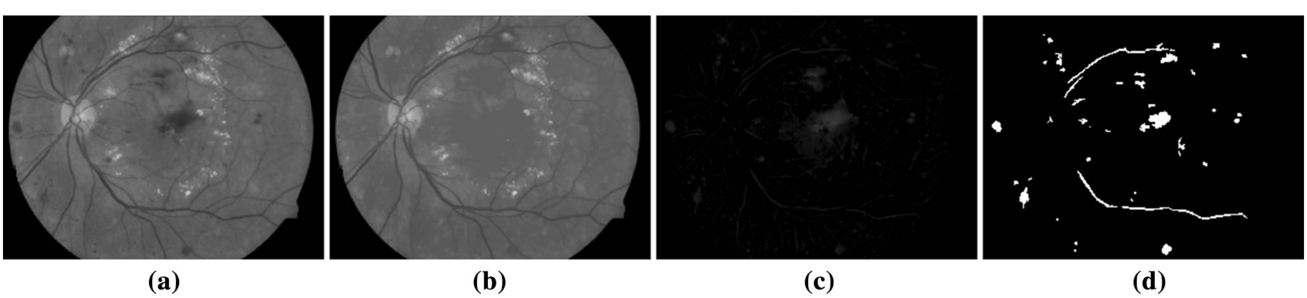

Fig. 9 Red lesions segmentation **a** shade-corrected green channel, **b** flood-fill operation, **c** subtraction of shade-corrected from filled image, **d** binarization of the subtracted image

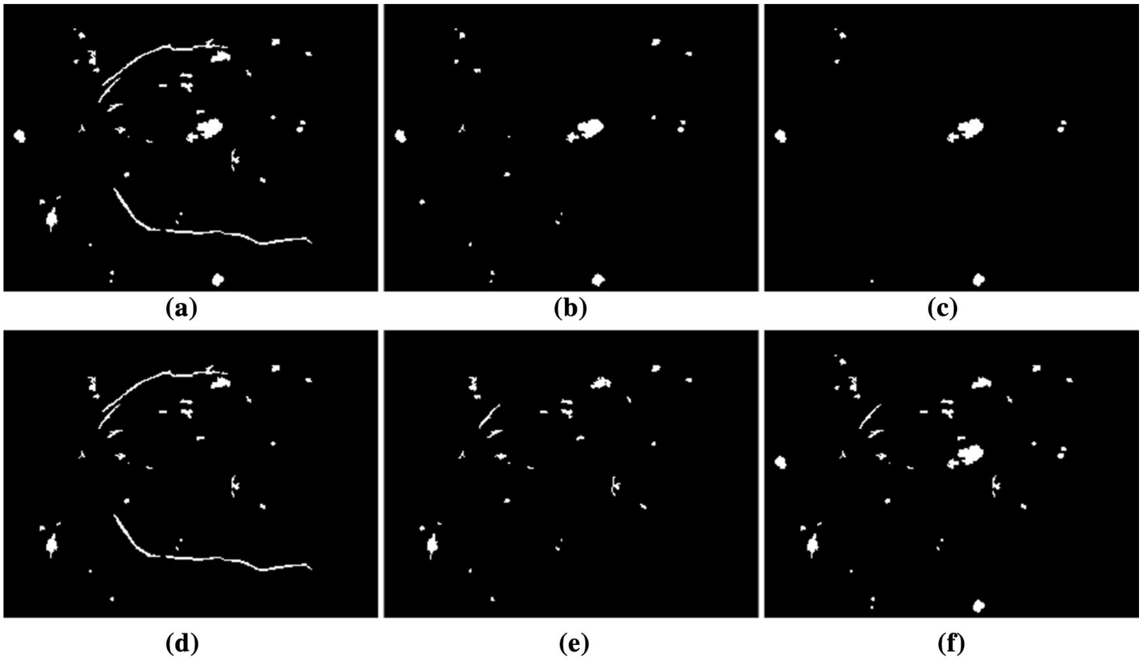

Fig. 10 Red lesions segmentation **a** candidate objects, **b** objects retained after major-to-minor axis ratio operation, **c** objects retained after intensity operation, **d** objects obtained by subtracting **c** from **a**, **e** objects retained post-circularity operation, **f** addition of **c** and **e** resulting in final red lesions detection

2.4 Framework for grading of disease

A framework to grade the severity of the disease has been used in the proposed work which is dependent on the quantitative analysis of bright and red lesions in the fundus image [19]. The framework used to grade the severity of disease is dependent on early treatment of diabetic retinopathy study (ETDRS) grading rule accepted by ophthalmologists. The following framework is considered in the proposed work:

(a) If no lesion is detected, then image is classified as NORMAL
(b) If red lesions detected are less than 5, then the image is classified as MILD
(c) If red lesions detected are between 5 and 10 (both values inclusive), then the image is classified as MODERATE
(d) If bright lesions are present, then the image is classified as SEVERE

3 Experimental results

The proposed algorithm has been tested on two distinct publicly available databases, namely DIARETDB1 and MESSIDOR. All the algorithms, optic disc segmentation, exudates segmentation and classification, red lesions segmentation, have been tested on images from both databases, and the results are found to be encouraging.

DIARETDB1 database [20] consists of 89 images out of which 84 images has signs of non-proliferative diabetic retinopathy (NPDR). The images were captured using a fundus camera with 50° field of view (FOV). The images contain some amount of imaging noises. The images have resolution of 1152 $\times$ 1500 pixels with bit depth of 24 bits and in PNG format. The database has ground truth available for the abnormalities present in the images.

MESSIDOR database [21] is a publicly available database for the study of diabetic retinopathy in fundus images. It is a huge database and consists of 1200 images. However, for the proposed work, 100 images have been considered for validation of the algorithm. The images have been captured using a fundus camera with 45° FOV. The images are coloured and have 8 bits per colour plane in TIFF format and have resolution of 2240 $\times$ 1488 pixels. The database consists of fundus images graded for diabetic retinopathy and diabetic macular oedema.

Figures 11 and 12 show the results obtained using the image processing algorithms proposed in the present work for DIARETDB1 and MESSIDOR databases, respectively. Figures 11a and 12a show the input image in RGB format. Figures 11b and 12b show the optic disc centre detected using the averaging filter and maximum intensity pixel identification method as proposed in the work. The optic disc and blood vessels present on it appears as noise to

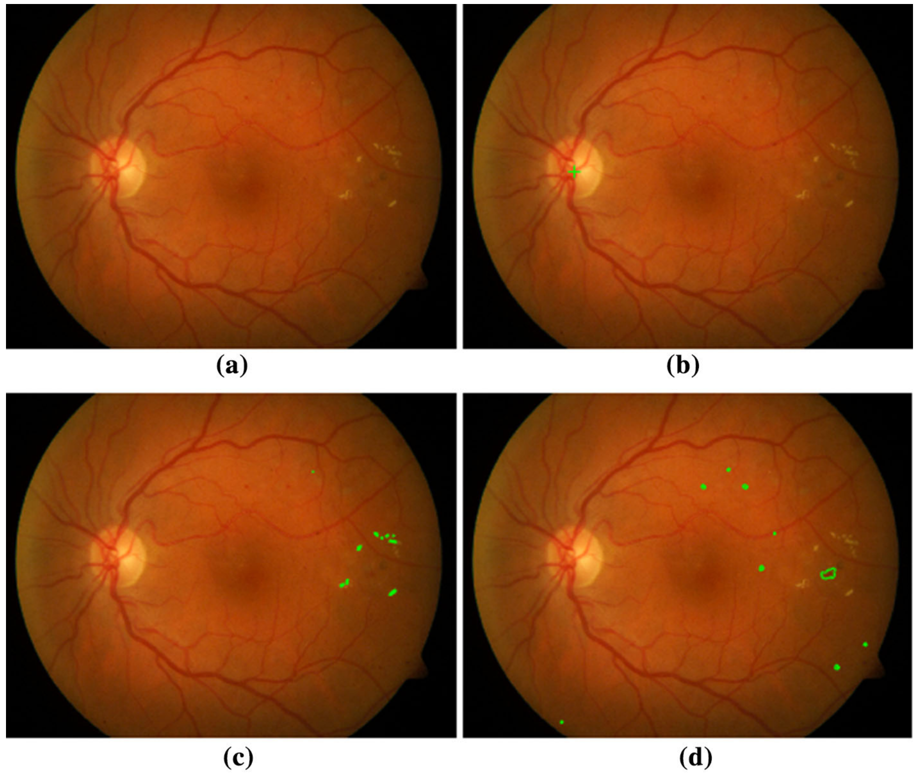

Fig. 11 Experimental results for DIARETDB1 database **a** input image, **b** optic disc centre marked on input image, **c** detected bright lesions marked on input image, **d** detected red lesions marked on input image

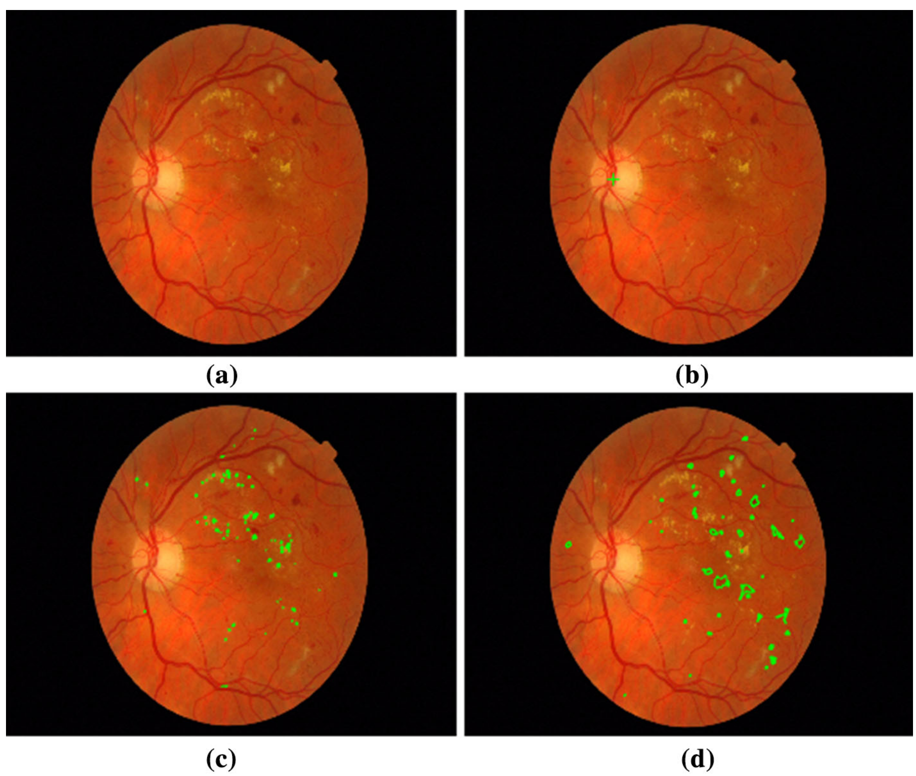

Fig. 12 Experimental results for MESSIDOR database **a** input image, **b** optic disc centre marked on input image, **c** detected bright lesions marked on input image, **d** detected red lesions marked on input image

exudates and red lesions, respectively. Hence, there arises a need to remove the optic disc from the image. A circle of certain radius around the detected disc centre is created and subtracted from the detected exudates and red lesion images. Figures 11c and 12c show the exudates detected in a fundus image using the proposed algorithm marked on the

Table 2 Performance measures obtained using proposed method

S no.	Database	Sensitivity (%)	Specificity (%)	Accuracy (%)
1	DIARETDB1	92.85	80.00	92.13
2	MESSIDOR	86.03	79.69	84.00

Table 3 Computation time elapsed using proposed method (seconds)

S no.	Database	Optic disc localization	Bright lesion segmentation	Bright lesion classification	Shade correction	Red lesion segmentation	Total time elapsed
1	DIARETDB1	1.7 ± 0.645	10 ± 0.23	15 ± 0.717	1.8 ± 0.665	2.2 ± 0.542	33 ± 0.499
2	MESSIDOR	2.1 ± 0.831	14 ± 0.459	21 ± 0.827	2.6 ± 0.475	2.9 ± 0.149	45 ± 0.341

input fundus image. The false positives are rejected with the help of a classification process which is based on statistical, geometrical and location-based features. Figures 11d and 12d show the detected red lesions marked on the input fundus image using proposed method. The false positives are removed using a geometrical and intensity-based framework. The figure shows the detected abnormalities for few samples from both databases.

The results for the proposed algorithm are presented using some performance parameters such as sensitivity, specificity and accuracy. Since the ground truth for pixel-wise segmentation is not available for both databases, an image-based performance analysis is reported. Sensitivity is a measure of classifying an unhealthy image, possessing signs of DR, as unhealthy. In the similar way, specificity is a measure of classifying a normal labelled image as normal. Accuracy is the average of both sensitivity and specificity.

Out of 89 images from the DIARETDB1 database, 84 images have signs of NPDR and five are normal images. Four out of five normal images were detected correctly as normal using the proposed algorithm which resulted in a specificity of 80%. Seventy-eight images were correctly classified as showing signs of NPDR. This resulted in a sensitivity of 92.85%. A total accuracy of 92.13% was obtained for DR detection using the proposed method.

The proposed method was tested for 200 images from MESSIDOR database which had 64 normal images, while 136 images possessed pathology related to NPDR. Using the proposed algorithm, 117 out of 136 unhealthy images showed signs of NPDR, while 51 out of 64 normal images were detected normal which resulted in a sensitivity and specificity of 86.03 and 79.69%, respectively. An accuracy of 84% was obtained for MESSIDOR database. The results for image-based performance analysis are reported in Table 2.

The proposed method has been developed and tested on a computing machine with MATLAB 2016a tool installed. The image processing and statistics and machine learning toolboxes of MATLAB tool were installed and mostly used for development of proposed algorithms. The computing machine had a processing unit clocking @ 2.5 GHz, 4 GB RAM and 64-bit operating system. The computation time involved in segmentation and detection of optic disc, and both types of lesions, is summarized in Table 3. An average time of 33 and 45 s took for complete grading of a fundus image for DR detection.

4 Conclusions

This work proposes a method for segmentation of optic disc, bright and red lesions from fundus images. These objects and abnormalities have been used strategically to analyse a fundus image for the presence of diabetic retinopathy. A quantitative analysis of the segmented lesions is done to grade the severity of the disease. The proposed methods have been tested on two varied databases and have resulted in good sensitivity and accuracy of DR detection. The proposed method is clinically significant as it is based on a globally accepted framework by ophthalmologists for grading the severity as mild, moderate and severe. The consideration of both types of lesions, i.e. bright and red, makes the proposed more robust and comprehensive for DR detection.

Acknowledgements This work was supported in part by the Grants from Department of Science and Technology, No. DST/TSG/ICT/2013/37. Also, the authors express their thankfulness to Dr. S. C. Gupta, Medical Director of Venu Eye Research Centre, for his kind support.

Compliance with ethical standards

Conflict of interest The authors declare that they have no conflict of interest.

References

1. Roychowdhury S, Koozekanani DD, Parhi KK (2014) DREAM: diabetic retinopathy analysis using machine learning. IEEE J Biomed Health Inf 18(5):1717–1728
2. Seoud L, Hurtut T, Chelbi J, Cheriet F, Langlois JMP (2016) Red lesion detection using dynamic shape features for diabetic retinopathy screening. IEEE Trans Med Imaging 35(4):1116–1126
3. Issac A, Sarathi MP, Dutta MK (2015) An adaptive threshold based image processing technique for improved glaucoma detection and classification. Comput Methods Programs Biomed 122(2):229–244
4. Franklin SW, Rajan SE (2014) Diagnosis of diabetic retinopathy by employing image processing technique to detect exudates in retinal images. IET Image Proc 8(10):601–609
5. Ranamuka NG, Meegama RGN (2013) Detection of hard exudates from diabetic retinopathy images using fuzzy logic. IET Image Proc 7(2):121–130
6. Sengar N, Dutta MK (2017) Automated system for detection and hierarchal grading of diabetic retinopathy. In: Computer methods in biomechanics and biomedical engineering: imaging and visualization. Taylor & Francis Publishers, pp 1–11
7. Antal B, Hajdu A (2012) An ensemble-based system for microaneurysm detection and diabetic retinopathy grading. IEEE Trans Biomed Eng 59(6):1720–1726
8. Ram K, Joshi GD, Sivaswamy J (2011) A successive clutter-rejection-based approach for early detection of diabetic retinopathy. IEEE Trans Biomed Eng 58(3):664–673
9. Parthasarathi M, Dutta MK, Singh A, Travieso CM (2016) Blood vessel inpainting based technique for efficient localization and segmentation of optic disc in digital fundus images. Biomed Signal Process Control 25:108–117. ISSN 1746-8094. https://doi.org/10.1016/j.bspc.2015.10.012
10. Singh A, Dutta MK, ParthaSarathi M, Uher V, Burget R (2016) Image processing based automatic diagnosis of glaucoma using wavelet features of segmented optic disc from fundus image. Comput Methods Programs Biomed 124:108–120
11. Yadav D, Sarathi MP, Dutta MK (2014) Classification of glaucoma based on texture features using neural networks. In: 7th international conference on contemporary computing (IC3), Noida, 2014, pp 109–112
12. Zhang L, Li Q, You J, Zhang D (2009) A modified matched filter with double-sided thresholding for screening proliferative diabetic retinopathy. IEEE Trans Inf Technol Biomed 13(4):528–534
13. Osareh A, Shadgar B, Markham R (2009) A computational-intelligence-based approach for detection of exudates in diabetic retinopathy images. IEEE Trans Inf Technol Biomed 13(4):535–545
14. Ganguly S et al (2014) An adaptive threshold based algorithm for detection of red lesions of diabetic retinopathy in a fundus image. In: International conference on medical imaging, m-health and emerging communication systems (MedCom), Greater Noida, 2014, pp 91–94
15. Dutta MK, ParthaSarathi M, Ganguly S, Ganguly S, Srivastava K (2017) An efficient image processing based technique for comprehensive detection and grading of non proliferative diabetic retinopathy from fundus images. Comput Methods Biomech Biomed Eng Imaging Vis 5(3):195–207
16. Soorya M, Issac A, Dutta MK (2018) An open source image processing algorithm for automated and robust glaucoma diagnosis from fundus images using novel blood vessel tracking and bend point detection. Int J Med Inf 110:52–70
17. Perona P, Malik J (1990) Scale-space and edge detection using anisotropic diffusion. IEEE Trans Pattern Anal Mach Intell 12(7):629–639
18. Liu J et al (2009) Photometric correction of retinal images by polynomial interpolation. In: 16th IEEE international conference on image processing (ICIP), Cairo, 2009, pp 3893–3896
19. Akram MU, Khalid S, Tariq A, Khan SA, Azam F (2014) Detection and classification of retinal lesions for grading of diabetic retinopathy. Comput Biol Med 45:161–171
20. Kauppi T, Kalesnykiene V, Kamarainen J-K, Lensu L, Sorri I, Raninen A, Voutilainen R, Uusitalo H, Kälviäinen H, Pietilä J (2007) DIARETDB1 diabetic retinopathy database and evaluation protocol. In: Proceedings of the 11th conference on medical image understanding and analysis, Aberystwyth, Wales, 2007
21. Decenciere E, Zhang X, Cazuguel G, Lay B, Cochener B, Trone C, Gain P, Ordonez R, Massin P, Erginay A, Charton B, Klein JC (2014) Feedback on a publicly distributed database: the Messidor database. Image Anal Stereol 33(3):231–234. ISSN 1854-5164